On the Use of Generalized DFT-s-OFDM to Reduce Inter-Numerology Interference in 5G-NR Networks

Gláucio P. Czekailo, Bruno S. Chang and Glauber Brante
CPGEI, Federal University of Technology - Paraná, Curitiba, Brazil
Email: glaucio@alunos.utfpr.edu.br, {bschang, gbrante}@utfpr.edu.br

***Abstract*— Orthogonal Frequency Division Multiplexing (OFDM) systems with a Cyclic Prefix (CP-OFDM) are the base waveform in fifth-generation New Radio (5G-NR) mobile networks, with the Discrete Fourier Transform precoded version (DFT-s-OFDM) as an alternative in Peak-to-Average Ratio (PAPR) limited scenarios. However, since 5G-NR networks use multiple numerologies, the coexistence of these numerologies introduces a novel non-orthogonality in the system, known as Inter-Numerology Interference (INI). The present work proposes an alternative to the use of the CP by means of the Generalized-Discrete Fourier Transform-spread-Orthogonal Frequency Division Multiplexing (G-DFT-s-OFDM) waveform. Our results show that the use of the G-DFT-s-OFDM waveform significantly reduces the INI in 5G-NR networks.**

***Keywords*— 5G-NR Networks, Inter Numerology Interference, Generalized DFT-s-OFDM.**

I. Introduction

3GPP in its Release 15 defined the complete structure for the physical layer of 5G New Radio (5G-NR) and its structural differences with respect to Long Term Evolution (LTE) [1], [2]. Their biggest difference relies on the support for multiple configurations in 5G-NR, by multiplexing different numerologies. The reason for this change is to provide flexibility, in order to support the distinct requirements of the 5G typical scenarios: enhanced Mobile BroadBand (eMBB), massive Machine-Type Communications (mMTC) and Ultra-Reliable Low Latency Communications (URLLC).

Orthogonal Frequency Division Multiplexing (OFDM) is a transmission technique that divides the available bandwidth into multiple subcarriers. In addition, the usage of a Cyclic Prefix (CP) in OFDM-based systems allows the use of simple (inverse) Fast Fourier Transforms ((I)FFTs), which reduces the complexity of the transceiver and equalization processes. Due to these factors, CP-OFDM has been used as a basic waveform in various radio technologies such as LTE, IEEE 802.11, and recently in 5G-NR.

A *numerology* defines parameters such as the allocated subcarrier spacing, OFDM symbol duration, CP duration, and slot duration for data channels [3]. In 5G-NR, a total of five numerologies are provided, with the conventional LTE numerology chosen as the base one. The base numerology considers a subcarrier spacing $\Delta_f = 15$ kHz, while the other numerologies are 2^μ multiples of Δ_f, with μ corresponding to the numerology index. These multiple numerologies provide flexibility, adapting each usage scenario to its demands in terms of bandwidth, robustness, *etc*.

However, the combination of CP-OFDM with multiple numerologies operating simultaneously results in a new type of interference, denoted as Inter-Numerology Interference (INI). That happens due to the loss of orthogonality between subcarriers of different numerologies in the frequency domain, as well as the difficulty in achieving symbol alignment in the time domain. At the same sampling rate, the FFT window of an OFDM symbol from one numerology does not align with the one from another numerology, making synchronization within the frame difficult. Discrete Fourier Transform - spread - OFDM (DFT-s-OFDM) schemes have been proposed in order to improve performance in Peak-to-Average Ratio (PAPR)-limited scenarios in 5G-NR [4]. Nevertheless, it has the same limitations of CP-OFDM regarding the INI, since a CP is also employed and the out-of-band (OOB) emissions are the same. Therefore, new strategies to reduce INI are welcome, and have been studied by the recent literature, *e.g.*, in [5]–[10].

Aiming to optimize network performance, the authors in [5] derive a closed-form expression of the INI in a DFT-s-OFDM system, in order to allocate power to the subcarriers as well as the numerology of each endpoint. In [6] a common CP for all numerologies is proposed, which minimizes the INI when compared with the standard individual CP used in 5G-NR. In [7] the OFDM transceiver is modified in order to use simple cyclic and frequency shift operations, designed to suppress the increase in the variance of the interference energy, by its turn reducing the INI effect. Furthermore, the authors in [8] propose a INI cancellation scheme, which employs a window in order to attenuate the side lobes of the FFT symbols, *i.e.*, serving as a filter to the system. Then, an analytical expression for the INI power is derived, which is a function of the frequency response of the interfering subcarrier channel, the spectral distance and the overlap windows generated by the sender and receiver windows.

In addition, in [9] the utilization of adaptive guards in time and frequency domains is shown as a solution to reduce the INI, along with a multi-window operation in the physical layer. An adaptive windowing operation is also used with a guard duration to reduce the unwanted emissions, together with a guard band to handle the INI level on the adjacent band. In [10], a pre-equalization method is proposed to remove the INI that occurs in multiple numerology OFDM frame structures on the transmitter side. The INI level can be also used as a parameter to create a model, as presented in [11], which can be used to build numerology profiles. As a consequence, one of the profiles can be adopted according to

the current users/traffic pattern, enhancing the performance of the system. In summary, the schemes proposed by [5]–[10] mainly deal with two approaches to handle the INI: filtering and different transmission strategies.

In this work, we present an alternative to DFT-s-OFDM in multi-numerology 5G-NR systems. Our proposal considers a generalized DFT-s-OFDM (G-DFT-s-OFDM) system [12], [13], which has better time and frequency localization when compared to the regular one, while being less complex than filtered systems such as the Generalized Frequency Division Multiplexing (GFDM), Universal Filtered MultiCarrier (UFMC) and Filter Bank Based Multicarrier (FBMC) [13]. This work presents simulations of G-DFT-s-OFDM operating in different scenarios, as well as a comparison with the conventional OFDM systems with a CP. Our results show that the use of G-DFT-s-OFDM is a valid and easy-to-implement alternative in multi-numerology 5G-NR, exhibiting much smaller INI values when compared to CP-OFDM. For instance, we show that it is possible to reduce the peak INI by at least 20 dB by using the G-DFT-s-OFDM. Moreover, the guard bands needed for a INI of -40 dB are at least 3.5 times smaller with respect to CP-OFDM systems. Finally, another important advantage is that G-DFT-s-OFDM maintains system compatibility, and it can actually be used along with DFT-s-OFDM/CP-OFDM if needed.

The remainder of this work is organized as follows: Section II explains INI in 5G-NR networks, while Section III presents the Generalized DFT-s-OFDM concept, its details, and the benefits of using G-DFT-s-OFDM systems in multi-numerology systems. Section IV shows and discusses the obtained INI results. Finally, Section V concludes this paper.

Notation: The identity matrix of size $N \times N$ is denoted by $\mathbf{I}_N$, while the all-zeros matrix of size $N \times N$ is denoted by $\mathbf{0}_N$. We use $M_{i,j}$ to refer to the $(i;j)$-th element of a matrix $\mathbf{M}$, and m_i to denote the i-th element of the vector $\mathbf{m}$.

II. Inter-Numerology Interference

The concept of multiple numerologies was designed to meet the needs of 5G-NR networks. This is due to the flexibility required in 5G applications, given the different requirements of eMBB, mMTC and URLLC scenarios. 5G-NR network numerologies are defined by [1], which establishes the structure for their data channels. Table I summarizes the parameters adopted by the 5 different numerologies of 5G-NR. A numerology μ is defined mainly by its subcarrier spacing Δ_f (in kHz), which in turn defines the bandwidth occupied by the Resource Block (RB). The RB in 5G defines the smallest contiguous transmission bandwidth that can be used, which is constructed by combining 12 subcarriers. Then, for a given subcarrier spacing Δ_f, the numerology defines an OFDM symbol period T_{OFDM} and a CP period T_{CP}, both in μs.

5G-NR networks are more flexible when compared to LTE because transmitters can operate simultaneously in more than one numerology. However, INI is one of the most important drawbacks of such simultaneous numerology usage. INI is caused by the loss of orthogonality between OFDM symbols, given that they now have different durations and subcarrier spacings. Such orthogonality loss occurs because of the CP added to each transmitted OFDM symbol. As an example, let us consider that symbols from two different numerologies, denoted by μ_1 and μ_2, are transmitted simultaneously. Let us also denote the symbol from numerology μ_1 as Narrow Subcarrier Spacing (NSCS), while the symbol from numerology μ_2 is the Wide Subcarrier Spacing (WSCS). If the ratio of their subcarrier spacings is, *e.g.*, $Q = \Delta_{\mu_2}/\Delta_{\mu_1} = 2$, then there will be one OFDM NSCS symbol being transmitted at the same time of two OFDM WSCS symbols. In addition, the CP causes a misalignment of the symbol position with respect to the FFT window, breaking the orthogonality among the multiple numerologies.

TABLE I:
Characteristics of 5G-NR Numerologies.

μ	Δ_f (kHz)	RB (kHz)	T_{OFDM} (μs)	T_{CP} (μs)
0	15	180	66.67	4.69
1	30	360	33.33	2.34
2	60	720	16.67	4.17l1.17
3	120	1440	8.33	0.58
4	240	2880	4.17	0.29

Moreover, transmitters using different subcarrier spacings will have different spectral sidelobe lengths. Nevertheless, it is known that OFDM sidelobes have high OOB emissions, which will require a large guard band between transmissions in order to reduce the INI to an acceptable level, without resorting to filtering or other transmission strategies. This also becomes an issue in mMTC scenarios, where transmissions are sporadic and may not be fully synchronized.

The organization of the 5G-NR transmitter takes into account that different numerologies will be transmitted simultaneously. Thus, in order to allocate the subcarrier indices in the IFFT in our example with two numerologies, a factor η is used as the subcarrier allocation ratio for the numerology with lower subcarrier spacing, while $1-\eta$ is the ratio for the numerology with larger subcarrier spacing. Figure 1 illustrates the difference between the NSCS and WSCS IFFT blocks in a scenario with $Q = 2$. For the scenario considered in this work, the first ηN subcarriers transmit data in the NSCS system, while the other ones are set to zero. On the other hand, the last $(1-\eta)N/Q$ subcarriers of the WSCS system transmit data, while the first $\eta N/Q$ ones are set to zero.

III. Generalized DFT-s-OFDM

G-DFT-s-OFDM replaces the CP by a head and tail, which share the subcarriers used by the transmitted data [13]. Thus, it is possible to generate the transmitted signal without losing the orthogonality among the numerologies. Another noteworthy benefit is the PAPR reduction, since the G-DFT-s-OFDM system inherits the low PAPR characteristic of DFT-s-OFDM. Finally, there is a significant reduction in OOB emissions when compared with CP-OFDM or DFT-s-OFDM systems [12], because G-DFT-s-OFDM has a known head and tail sequence, yielding a smooth transition between adjacent time symbols.

Figure 2 illustrates the G-DFT-s-OFDM transmitter. The guard head/tail can be defined as either with almost zero

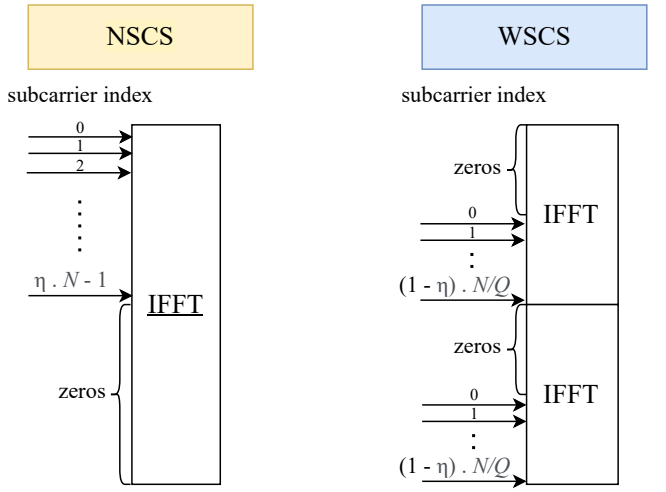

Fig. 1: Transmission strategies for NSCS and WSCS systems.

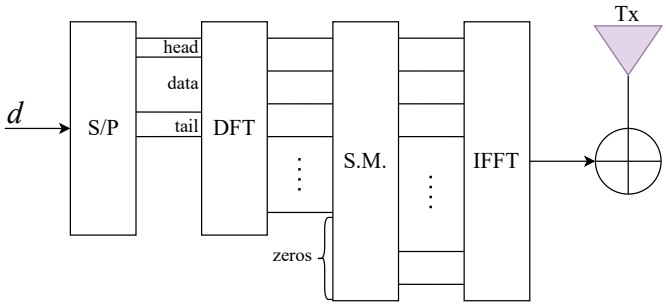

Fig. 2: G-DFT-s-OFDM transmitter scheme.

power, denoted by Zero-Tail (ZT) DFT-s-OFDM, or by containing a known sequence, denoted by Unique Word (UW) DFT-s-OFDM. In both cases, increasing the head/tail period decreases the amount of data to be transmitted. This is different from CP-OFDM, which has a fixed number of data subcarriers per symbol. Indeed, this property is responsible for maintaining the orthogonality of the FFTs in G-DFT-s-OFDM.

The transmitted signal in a G-DFT-s-OFDM system is given by a head $\mathbf{s}_h$ with length L_h, a tail $\mathbf{s}_t$ with length L_t, and the data $\mathbf{d}$ with length $N - L_h - L_t$. These samples are concatenated forming $\mathbf{q}$ with size N, which is expressed as

$$\mathbf{q} = [\mathbf{s}_h \quad \mathbf{d} \quad \mathbf{s}_t]. \tag{1}$$

The sizes of L_h and L_t are tuned by taking into account the desired OOB emissions and the length of the impulse response of the fading channel. Here, since our focus is only on the INI reduction, the fading channel is not considered in our analysis.

Then, $\mathbf{q}$ passes through a normalized FFT $\mathbf{F}_N$ with size $N \times N$, which has its output $\mathbf{t}$ mapped to frequency subcarriers through a mapping scheme $\mathbf{M}$ with size $N_{\text{FFT}} \times N$, generating $\mathbf{c}$ with length N_{FFT}. For the sake of simplicity and convenience, localized mapping is considered in our scenario, and $\eta = N/N_{\text{FFT}}$. The mapped signal $\mathbf{c}$ is processed by an IFFT $\mathbf{F}_{N_{\text{FFT}}}^{-1}$ with size $N_{\text{FFT}} \times N_{\text{FFT}}$, resulting in $\mathbf{y}$, which is the transmitter output. Thus, the transmitted signal $\mathbf{y}$ with length N_{FFT} can be expressed as

$$\mathbf{y} = \mathbf{F}_{N_{\text{FFT}}}^{-1} \mathbf{M} \mathbf{F}_N \, \mathbf{q}. \tag{2}$$

The receiver must act inversely with respect to the transmitter to obtain the data estimate. Therefore, its structure is composed of an FFT block, which has its output demapped into subcarriers that are processed by an IDFT. This sequence of steps results in the estimated signal composed of head, data, and tail. So, by discarding head and tail from the received signal, the estimated data is obtained. Thus, the receiver output $\hat{\mathbf{q}}$, without noise and channel fading, is given by

$$\hat{\mathbf{q}} = \mathbf{F}_N^{-1} \mathbf{M} \, \mathbf{F}_{N_{\text{FFT}}} \, \mathbf{r}, \tag{3}$$

where $\mathbf{r}$ is the received signal. As the generalized DFT signal $\mathbf{q}$ is composed of head, data, and tail, it is necessary to discard the head and tail sequences in order to obtain the symbol estimate at the receiver $\hat{\mathbf{d}}$, which can be done as $\hat{\mathbf{d}} = \mathbf{q}[N_h : (N - N_t - 1)]$.

Considering the scenario where G-DFT-s-OFDM symbols from an NSCS numerology $\mathbf{y}_n$, with length N_n, are transmitted together with Q G-DFT-s-OFDM symbols from a WSCS numerology $\mathbf{y}_w$, the overall transmitted signal $\mathbf{y}_o$ is

$$\mathbf{y}_o = \mathbf{y}_n + \mathbf{y}_w, \tag{4}$$

where $\mathbf{y}_w = [\mathbf{y}_{w,1} \ \ldots \ \mathbf{y}_{w,Q}]$ and $\mathbf{y}_{w,i}$ is the i-th WSCS symbol, with length $N_w = N_n/Q$. At the NSCS receiver, and considering a scenario without both noise and fading channel, the N_n-length signal $\mathbf{r}_n$ for the NSCS case is given by

$$\mathbf{r}_n = \mathbf{y}_n + \mathbf{y}_{\text{INI},w}, \tag{5}$$

where $\mathbf{y}_n$ is the desired signal and $\mathbf{y}_{\text{INI},w}$ is the INI caused by the WSCS symbols, both with length N_n. Likewise, $\mathbf{y}_{\text{INI},w}$ can be expressed as

$$\mathbf{y}_{\text{INI},w} = \mathbf{F}_{N_n} \mathbf{c}_w, \tag{6}$$

where $\mathbf{c}_w$ is the mapped signal from the WSCS transmitter. This mismatch between the FFT size employed at the NSCS receiver and the WSCS symbols generated by a transmitter employing a different FFT size is what causes the INI.

On the other hand, for the WSCS case the N_w-length signal $\mathbf{r}_{w,i}$ for the i-th symbol can be expressed as

$$\mathbf{r}_{w,i} = \mathbf{y}_{w,i} + \mathbf{y}_{\text{INI},n}, \tag{7}$$

where $\mathbf{y}_{w,i}$ is the desired WSCS signal and $\mathbf{y}_{\text{INI},n}$ is the domain INI caused by the NSCS signal, both with length N_w. In addition, $\mathbf{y}_{\text{INI},n}$ is given by

$$\mathbf{y}_{\text{INI},n} = \mathbf{F}_{N_w} \mathbf{c}'_n, \tag{8}$$

where $\mathbf{c}'_n$ is the vector corresponding to the samples of the mapped NSCS signal $\mathbf{c}_n$ that fall into the N_w length window of the WSCS receiver. Again, the mismatch between the FFT size employed at the WSCS receiver and the NSCS symbol generated by a transmitter employing a different FFT size is what causes the INI.

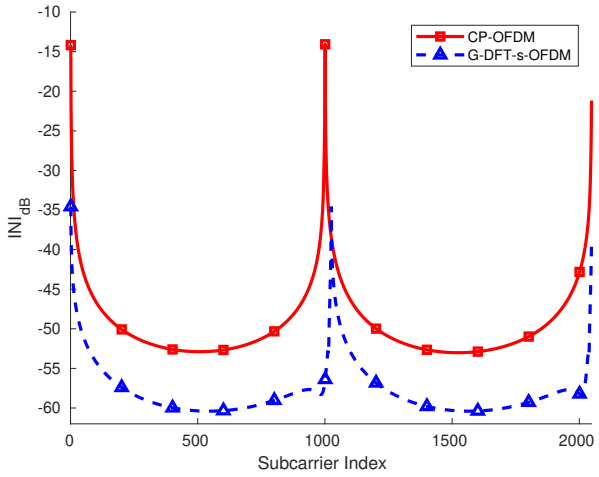

Fig. 3: INI of the G-DFT-s-OFDM and CP-OFDM schemes on the NSCS numerology for $Q = 2$.

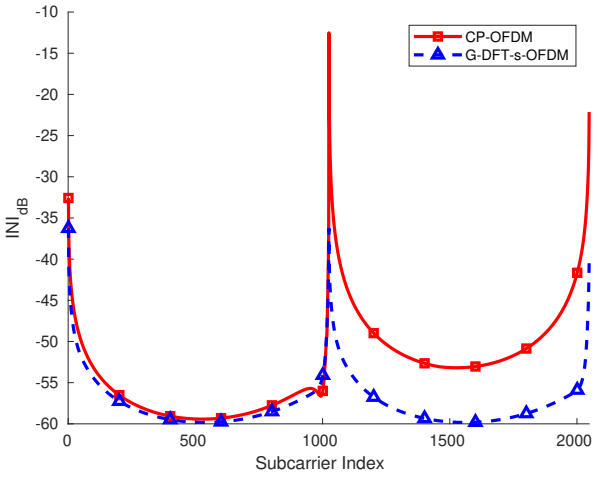

Fig. 4: INI of the G-DFT-s-OFDM and CP-OFDM schemes on the WSCS numerology for $Q = 2$.

IV. Simulation Results

With the aim of evaluating the INI reduction performance of the G-DFT-s-OFDM with respect to the regular CP-OFDM systems, a simulation model was developed. Transmitted data was drawn from binary phase shift keying (BPSK) modulated symbols with unit power. In addition, $Q \in \{2, 4, 8\}$ was considered and the base numerology (with $\Delta_{\mu_0} = 15$ kHz) is always the NSCS for the sake of simplicity, since the ratio between the subcarrier spacings from different numerologies is the determinant factor in INI [3]. The head length is $L_h = 16$ subcarriers, whereas the tail length is $L_t = 80$ subcarriers. ZT G-DFT-s-OFDM was considered without loss of generality, since its OOB emissions are the same as in UW G-DFT-s-OFDM [13]. The total number of subcarriers is $N = 4096$ for the lower numerology scenario, and only two simultaneous numerologies are considered, denoted by NSCS and WSCS, where $\eta = 0.5$. For the CP-OFDM system, the CP length is the sum of head and tail lengths, so that $L_{\text{CP}} = 96$. Additionally, only one RB per symbol was activated in order to analyze the impact of its INI in the entire system.

The INI experienced by the NSCS symbol for $Q = 2$ is illustrated in Figure 3. Due to the time misalignment between symbols the highest INI levels are observed at the symbol transition. In the CP-OFDM case, due to the CP length the symbol transition on WSCS happens before subcarrier 1024, which the is the middle subcarrier of this numerology for $\eta = 0.5$, $N = 2048$ and consequently $Q = 2$. This brings the INI peak about 15 subcarrier indexes to the left. In the G-DFT-s-OFDM system the alignment is not disturbed by the CP, making the peak of INI being observed at the middle of the NSCS symbol (subcarrier number 1024). More importantly, we observe that the INI peak with G-DFT-s-OFDM at this transition is at approximately -35 dB, which is 20 dB lower than that obtained in the CP-OFDM case.

Figure 4 presents the INI experienced by the Q symbols from the WSCS numerology and $Q = 2$. In the CP-OFDM case, the first symbol experiences the same INI as the one from G-DFT-s-OFDM systems, due to the position of the interfering RB on the NSCS system affecting only the second symbol from the WSCS system. However, in the case of G-DFT-s-OFDM the INI peak for the WSCS numerology at the symbol transition is at approximately -37 dB, which is 25 dB lower when compared to the CP-OFDM system.

In order to compare the performance of CP-OFDM and G-DFT-s-OFDM systems regarding the INI decay at the neighbor subcarriers of each numerology, the number of guard band subcarriers to reach INI levels of -40 and -50 dB was chosen as a benchmark. Table II compares the guard band required for CP-OFDM and G-DFT-s-OFDM according to the type of numerology (NSCS or WSCS). We observe that the G-DFT-s-OFDM system requires a much smaller number of subcarriers to achieve the same INI level of CP-OFDM, evidencing that the use of G-DFT-s-OFDM is beneficial for 5G-NR networks in terms of spectral efficiency. As an example, to obtain INI $= -40$ dB for NSCS in this scenario, a guard band of 420 kHz is needed in CP-OFDM systems, whereas a guard band of only 30 kHz is needed for G-DFT-s-OFDM. If the INI threshold is of -50 dB, a guard band of almost 3 MHz is needed in CP-OFDM systems, whereas a guard band of only 135 kHz (22 times smaller) is needed for G-DFT-s-OFDM.

Higher values of Q are relevant scenarios due to their usability in real world conditions, allowing higher order numerologies to coexist closely with ones containing smaller subcarrier spacings. Figures 5 and 6 show the INI for WSCS and NSCS signals, respectively, with $Q \in \{2, 4, 8\}$ for both G-DFT-s-OFDM and CP-OFDM schemes. As we observe, when Q is high the INI peaks of the G-DFT-s-OFDM systems are also lower than that of the CP-OFDM, for both WSCS and

TABLE II: Number of subcarriers needed to reach a given level of INI for $Q = 2$.

Numerology	Scheme	INI $= -40$ dB	INI $= -50$dB
NSCS	CP-OFDM	28	199
	G-DFT-s-OFDM	2	9
WSCS	CP-OFDM	36	210
	G-DFT-s-OFDM	1	11

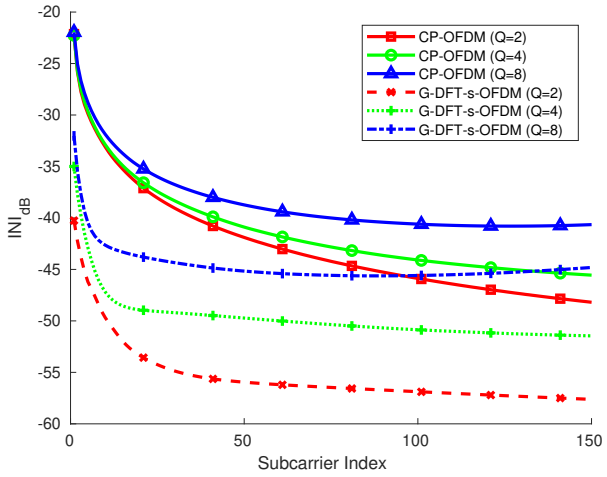

Fig. 5: INI on the edge subcarriers for WSCS numerology for $Q \in \{2, 4, 8\}$.

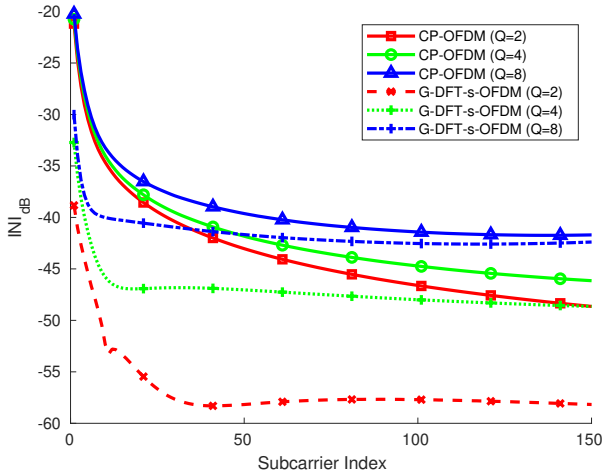

Fig. 6: INI on the edge subcarriers for NSCS numerology for $Q \in \{2, 4, 8\}$.

TABLE III: Number of subcarriers needed to reach INI $= -40$ dB with $Q = 4$ and 8.

Numerology	Scheme	$Q = 4$	$Q = 8$
NSCS	CP-OFDM	34	57
	G-DFT-s-OFDM	5	10
WSCS	CP-OFDM	27	43
	G-DFT-s-OFDM	5	12

NSCS numerologies, with a reduction of approximately 13 dB for $Q = 4$ and 9 dB for $Q = 8$ when using G-DFT-s-OFDM instead of CP-OFDM. Finally, Table III compares G-DFT-s-OFDM and CP-OFDM in terms of the number of subcarriers needed to obtain a level of INI $= -40$ dB, with $Q = 4$ and $Q = 8$. G-DFT-s-OFDM requires a much smaller guard band to achieve the same INI level of CP-OFDM. For instance, with $Q = 4$, the guard band of G-DFT-s-OFDM is approximately 1.74 MHz smaller than that of CP-OFDM in NSCS, with the difference being of 1.32 MHz in WSCS. Such gap increases respectively to 5.64 and 3.72 MHz with $Q = 8$.

V. Conclusion

In this work we have presented the usage, benefits and INI comparison results for the G-DFT-s-OFDM waveform on 5G-NR networks. Since the DFT-s-OFDM scheme is already used on 5G-NR, the replacement of the CP by a flexible head and tail that fit the symbols duration is a compatible new way, which is shown to greatly reduce the INI observed in 5G-NR systems and improve their spectral efficiency by reducing the guard bands. As future extensions, we propose more complex interference cancellation schemes in order to further reduce the INI, such as the successive interference cancellation scheme, as well as extend it to multiple antenna systems. Other suggestions are a theoretical derivation of the INI obtained with G-DFT-s-OFDM systems and a comparison with DFT precoded filter bank systems [14].

Acknowledgment

This work has been supported by CAPES, Finance Code 001, and CNPq.

References

[1] 3rd Generation Partnership Project (3GPP), "NR - physical channels and modulation (release 15)," *Technical Specification 38.211, ver 15.1.0*, april 2018.

[2] ——, "NR - Base Station (BS) radio transmission and reception (release 15)," *Technical Specification 38.104, ver 15.1.0*, april 2018.

[3] D. Demmer, R. Gerzaguet, J.-B. Dore, and D. Le Ruyet, "Analytical study of 5G NR eMBB co-existence," in *25th International Conference on Telecommunications (ICT)*, 2018, pp. 186–190.

[4] H. G. Myung, J. Lim, and D. J. Goodman, "Single carrier FDMA for uplink wireless transmission," *IEEE Vehicular Technology Magazine*, vol. 1, no. 3, pp. 30–38, 2006.

[5] F. Lotfi and O. Semiari, "Performance analysis and optimization of uplink cellular networks with flexible frame structure," in *IEEE 93rd Vehicular Technology Conference (VTC2021-Spring)*, 2021, pp. 1–5.

[6] A. B. Kihero, M. S. J. Solaija, and H. Arslan, "Inter-numerology interference for beyond 5G," *IEEE Access*, vol. 7, pp. 146 512–146 523, 2019.

[7] J. Choi, B. Kim, K. Lee, and D. Hong, "A transceiver design for spectrum sharing in mixed numerology environments," *IEEE Transactions on Wireless Communications*, vol. 18, no. 5, pp. 2707–2721, 2019.

[8] X. Zhang, L. Zhang, P. Xiao, D. Ma, J. Wei, and Y. Xin, "Mixed numerologies interference analysis and inter-numerology interference cancellation for windowed OFDM systems," *IEEE Transactions on Vehicular Technology*, vol. 67, no. 8, pp. 7047–7061, 2018.

[9] A. F. Demir and H. Arslan, "Inter-numerology interference management with adaptive guards: A cross-layer approach," *IEEE Access*, vol. 8, pp. 30 378–30 386, 2020.

[10] B. A. Cevikgibi, A. M. Demirtas, T. Girici, and H. Arslan, "Inter-numerology interference pre-equalization for 5G mixed-numerology communications," *arXiv preprint arXiv:2201.09228*, 2022.

[11] N. Correia, F. Al-Tam, and J. Rodriguez, "Optimization of mixed numerology profiles for 5G wireless communication scenarios," *Sensors*, vol. 21, no. 4, p. 1494, 2021.

[12] G. Berardinelli, K. I. Pedersen, T. B. Sorensen, and P. Mogensen, "Generalized DFT-spread-OFDM as 5G waveform," *IEEE Communications Magazine*, vol. 54, no. 11, pp. 99–105, 2016.

[13] G. Berardinelli, "Generalized DFT-s-OFDM waveforms without cyclic prefix," *IEEE Access*, vol. 6, pp. 4677–4689, 2017.

[14] R. P. Junior, C. A. F. d. Rocha, B. S. Chang, and D. Le Ruyet, "A novel DFT precoded filter bank system with iterative equalization," *IEEE Wireless Communications Letters*, vol. 10, no. 3, pp. 478–482, 2021.